Time-Resolved Charge Translocation by Sarcoplasmic Reticulum Ca-ATPase Measured on a Solid Supported Membrane

Francesco Tadini Buoninsegni,* Gianluca Bartolommei,* Maria Rosa Moncelli,* Giuseppe Inesi,† and Rolando Guidelli*

*Department of Chemistry, University of Florence, 50019 Sesto Fiorentino, Italy; and †Department of Biochemistry and Molecular Biology, University of Maryland School of Medicine, Baltimore, Maryland 21201 USA

ABSTRACT Sarcoplasmic reticulum vesicles were adsorbed on an octadecanethiol/phosphatidylcholine mixed bilayer anchored to a gold electrode, and the Ca-ATPase contained in the vesicles was activated by ATP concentration jumps both in the absence and in the presence of K^+ ions and at different pH values. Ca^{2+} concentration jumps in the absence of ATP were also carried out. The resulting capacitive current transients were analyzed together with the charge under the transients. The relaxation time constants of the current transients were interpreted on the basis of an equivalent circuit. The current transient after ATP concentration jumps and the charge after Ca^{2+} concentration jumps in the absence of ATP exhibit almost the same dependence upon the Ca^{2+} concentration, with a half-saturating value of $\sim$1.5 μM. The pH dependence of the charge after Ca^{2+} translocation demonstrates the occurrence of one H^+ per one Ca^{2+} countertransport at pH 7 by direct charge-transfer measurements. The presence of K^+ decreases the magnitude of the current transients without altering their shape; this decrease is explained by K^+ binding to the cytoplasmic side of the pump in the E_1 conformation and being released to the same side during the E_1–E_2 transition.

INTRODUCTION

The Ca-ATPase of the sarcoplasmic reticulum (SR) is an integral membrane protein that couples the hydrolysis of a molecule of ATP to the active transport of two Ca^{2+} ions across the membrane of SR (Møller et al., 1996; Lee and East, 2001). It plays an essential role in regulating intracellular calcium concentration, which is kept at or below 0.1 μM by pumping ions from the cytoplasm into the SR lumen: in this manner, SR Ca-ATPase induces muscle relaxation, contributing to calcium homeostasis. Reduced activity of this pump may result in prolonged elevated calcium levels, which may lead to stiffness and muscle relaxation problems (Gommans et al., 2002; MacLennan, 2000).

Like other members of the P-type ATPases class, Ca-ATPase forms an aspartyl-phosphate intermediate during the enzymatic reaction cycle. According to the E_1–E_2 model, Ca^{2+} binding to the cytosolic domain in the high-affinity E_1 conformation is followed by the phosphorylation of an aspartyl residue (Asp-351) by ATP. A conformational change of the phosphoenzyme from the E_1P to the E_2P state exposes Ca^{2+} to the lumenal side and promotes Ca^{2+} release, due to the low Ca^{2+} affinity for the E_2P state of the pump. After the cleavage of the phosphoenzyme, the pump returns to the E_1 conformational state (Carafoli and Brini, 2000). The recent availability of the crystal structure of SR Ca-ATPase, both in the E_1Ca_2 conformation (Toyoshima et al., 2000) and in the E_2 conformation stabilized by thapsigargin (Toyoshima and Nomura, 2002), has represented a breakthrough in the understanding of structure-function relationships (Lee and East, 2001; Hua et al., 2002).

From functional studies, Ca^{2+} binding to Ca-ATPase was found to be electrogenic (Butscher et al., 1999). Kinetic studies have shown that under physiological conditions Ca-ATPase couples the translocation of two Ca^{2+} ions to the countertransport of two protons (Yu et al., 1993, 1994). However, the Ca^{2+}/H^+ stoichiometry changes when the cytoplasmic pH is varied at constant lumenal pH or when the lumenal pH is varied at constant cytoplasmic pH (Yu et al., 1994).

Potassium ion was reported to influence the pumping activity of Ca-ATPase in different ways. The construction of chimeric ATPases between Na,K-ATPase and Ca-ATPase revealed two distinct regions with different K^+ affinity (Ishii et al., 1997; Yoshimura et al., 1997). A potassium binding site that induces a decrease in Ca^{2+} affinity for the pump, when occupied by K^+ ions, was proposed by Lee et al. (1995) on the basis of kinetic studies. A competition of K^+ with Ca^{2+} for the Ca^{2+} binding site less exposed to the cytoplasm was also postulated (Lee et al., 1995). Potassium ion was also reported to accelerate the decomposition of the ADP-insensitive form of the enzyme (Yamada and Ikemoto, 1980) and the slow component of the biphasic fluorescence signal due to Ca^{2+} binding, when in the presence of Mg^{2+} (Moutin and Dupont, 1991).

Presteady-state electrical measurements of the activity of an ion pump yield direct information about the time dependence of the charge movement across the pump (Läuger, 1991; Pintschovius and Fendler, 1999). Adsorbing

Submitted November 3, 2003, and accepted for publication March 1, 2004.

Address reprint requests to Prof. Rolando Guidelli, Dept. of Chemistry, University of Florence, via della Lastruccia 3, 50019 Sesto Fiorentino, Italy. Tel.: 39-055-4573097; Fax: 39-055-4573098; E-mail: guidelli@unifi.it.

0006-3495/04/06/3671/16 $2.00

doi: 10.1529/biophysj.103.036608

membrane fragments or proteoliposomes on a conventional black lipid membrane (BLM) (Hartung et al., 1987, 1997) or on a derivatized solid support (Pintschovius and Fendler, 1999) and activating them by a concentration jump causes a certain distortion of the pump current, due to the combined support-membrane system; this, however, can be satisfactorily accounted for. A convenient method to perform concentration jumps of an arbitrary substrate at the surface of a solid-supported membrane (SSM) was devised by Pintschovius and Fendler (1999). The SSM consists of an alkanethiol monolayer firmly anchored to a gold surface via the sulfhydryl group, with a second phospholipid monolayer on top of it. Membrane fragments or proteoliposomes are then adsorbed on this gold-supported mixed thiol-lipid bilayer. This technique combines the high mechanical stability of the SSM with a rapid solution exchange procedure. This method has been successfully used to investigate the electrogenic partial reactions in the enzymatic cycle of Na,K-ATPase (Pintschovius and Fendler, 1999; Pintschovius et al., 1999; Tadini Buoninsegni et al., 2000; Tadini Buoninsegni et al., 2003) and the charge transfer of the melibiose permease (Ganea et al., 2001).

This study describes an application of the SSM technique to the investigation of the pumping activity of SR Ca-ATPase. SR vesicles containing ATPase from rabbit skeletal muscle were adsorbed on the SSM. Upon adsorption, the ion pumps were activated by ATP concentration jumps at variable ATP concentration, Ca^{2+} concentration, and pH, and the current transients generated by Ca-ATPase activity were measured under potentiostatic conditions. Ca^{2+} concentration jumps in the absence of ATP were also carried out, to investigate Ca^{2+} binding to and release from the pump. Finally, the influence of the presence of physiological concentrations of K^+ ions on the Ca-ATPase pumping activity was studied.

MATERIALS AND METHODS

Chemicals

Calcium, potassium and magnesium chlorides, and Tris were obtained from Merck (Darmstadt, Germany) at analytical grade. Adenosine-5′-triphosphate disodium salt (ATP, ~97%) and dithiothreitol (DTT, ≥99%) were purchased from Fluka (Buchs, Switzerland). Octadecanethiol (98%) from Sigma-Aldrich (St. Louis, MO) was used without further purification. EGTA, tetraethylammonium chloride (TEA, 98%), thapsigargin, and calcimycin (calcium ionophore A23187) were obtained from Sigma-Aldrich. Protonophore 1799, (2,6-dihydroxy)-1,1,1,7,7,7-hexafluoro-2,6-bis(trifluoro-methyl)heptane-4-one, was kindly provided by the Max-Planck-Institüt für Biophysik.

The lipid solution contained diphytanoylphosphatidylcholine (Avanti Polar Lipids, Alabaster, AL) and octadecylamine (puriss., Fluka) (60:1) and was prepared at a concentration of 1.5% (w/v) in *n*-decane (Merck) as described by Bamberg et al. (1979).

Sarcoplasmic reticulum vesicles were obtained by extraction from the fast twitch hind leg muscle of New Zealand white rabbit, followed by homogenization and differential centrifugation, as described by Eletr and Inesi (1972). The vesicles so obtained, derived from longitudinal SR membrane, contained only negligible amounts of the ryanodine receptor Ca^{2+} channel associated with junctional SR (light vesicles). The protein/lipid ratio was 1:1 and the total protein content was 22.4 mg/ml, of which ~50% consisting of Ca-ATPase.

The free calcium concentration was calculated with the computer program Winmaxc v. 2.40 (Bers et al., 1994). Unless otherwise stated, 1 μM calcium ionophore A23187 was used to prevent Ca^{2+} accumulation inside the vesicles (Hartung et al., 1997).

The solid supported membrane

The SSM consisted of an alkanethiol monolayer covalently bound to a gold surface via the sulfur atom, with a phospholipid monolayer on top of it (Seifert et al., 1993; Florin and Gaub, 1993). To prepare the SSM, the procedure described by Pintschovius and Fendler (1999) was followed. Briefly, the mixed bilayer was formed in two sequential self-assembly steps. A self-assembled octadecanethiol monolayer was first formed on a gold electrode by incubating a freshly deposited gold film in an ethanol solution of 1 mM octadecanethiol for 6 h at room temperature. The bilayer was then formed by spreading a drop of lipid solution (usually 5 μl) on the surface of the thiol-coated gold electrode. Typically, the effective membrane area ranged from 2 to 3 mm^2.

Setup

To carry out rapid concentration jumps, a Plexiglas cuvette with an inner volume of 20 μl was used. The SSM and an O-ring, which contained the actual solution volume, were sandwiched between the upper and the lower part of the cuvette. The SSM acted as the working electrode, while an Ag/AgCl(0.1M KCl) electrode was employed as a counterelectrode. The counterelectrode was separated from the streaming solution by an agar/agar gel bridge. For details, see Pintschovius and Fendler (1999).

Two different 100 ml glass containers were used for the nonactivating and the activating solution. Unless otherwise stated, the activating solution differed from the nonactivating one only by the presence of the species activating the pump or binding to it. When performing a concentration-jump experiment, the solution flow was kept constant at ~60 ml/min by applying a pressure of 0.4 bar to the system and by controlling the pressure with a precision digital manometer. The cuvette was connected to the outlet of a Teflon block on which two solenoid valves were mounted (model 225T052, NResearch, West Caldwell, NJ). The two valves, which were computer controlled through a digital-to-analog converter (DAC 488/2, IOtech, Cleveland, OH), allowed a fast switching between the activating and the nonactivating solution. All parts of the setup conducting the electrolyte solutions were enclosed in a Faraday cage. The current, generated by the ion pumps upon keeping the applied potential between the SSM and the counterelectrode equal to zero, was amplified by a current amplifier (Keithley (Cleveland, OH) 428, gain: 10^9 V/A), filtered (low-pass, 3 ms), recorded (16-bit analog-to-digital converter, IOtech ADC 488/8SA), visualized (Oscilloscope, Tektronix (Beaverton, OR) TDS 340A) and stored (Power PC G3, Macintosh, Apple, Cupertino, CA). Operation of the experimental setup and data acquisition were carried out under computer control (GPIB interface, National Instruments (Austin, TX) board) using a homemade acquisition program written in LabView (National Instruments) environment.

Solution exchange technique

Two hours after forming the SSM and filling the cuvette, the capacitance and conductance of the SSM remained constant at $C_m = 0.2–0.4$ $\mu F/cm^2$ and $G_m = 50–100$ nS/cm^2. At this stage of the procedure, control experiments were usually performed with the protein-free SSM to exclude any artifacts generated by the solution exchange (Pintschovius and Fendler, 1999). The SR vesicles containing Ca-ATPase were then added by injecting 20 μl of their suspension into the cuvette through the outlet opening. The suspension

was then vigorously mixed using a pipette. The vesicles were adsorbed on the SSM for 30 min upon applying a potential difference of +0.1 V. The usual procedure for a concentration-jump experiment consisted of three steps: i), washing the cuvette with the nonactivating solution for 1 s; ii), injecting the activating solution into the cuvette for 1 s; and iii), removing the activating solution from the cuvette with the nonactivating solution for 1 s.

To verify the reproducibility of the current transients generated within the same set of measurements on the same SSM, each single measurement of the set was repeated 4–5 times and then averaged to improve the signal/noise ratio. Average standard deviations were usually found to be no $>\pm 5\%$. At the beginning of each set of measurements, 100 μM ATP jumps were carried out to test the activity of the ion pump previously adsorbed on the gold-supported alkanethiol/phospholipid mixed bilayer. The same ATP jump was performed at the end of the set of measurements, and the initial and final ATP-induced current transients were then compared to rule out any loss of activity during the time of the experiment. If differences between the two transients were $>\pm 5\%$, the set was discarded.

RESULTS

Electrical currents generated by Ca-ATPase were measured by adsorbing native vesicles containing Ca-ATPase from rabbit skeletal muscle on the SSM. The calcium pumps were then activated under different experimental conditions.

Different ATP concentration jumps at a constant, saturating Ca^{2+} concentration

Fig. 1 shows a typical potentiostatic current transient after a 100 μM ATP concentration jump in the presence of a free calcium concentration of 100 μM. The sign of the current peak is negative and corresponds to the transport of positive charge from the aqueous solution toward the SSM (Dolfi et al., 2002). The direction of the current indicates that the native vesicles containing Ca-ATPase that contribute to the electrical signal are adsorbed with the cytoplasmic side facing the aqueous solution.

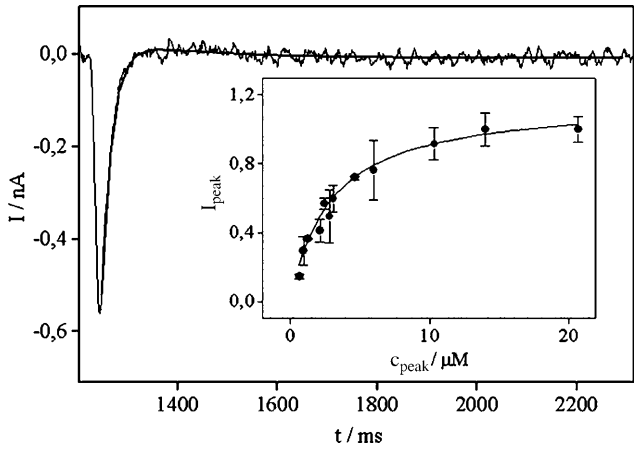

FIGURE 1 Current transient after an ATP concentration jump obtained with a nonactivating solution containing 150 mM choline chloride, 1 mM $MgCl_2$, 1.1 mM $CaCl_2$ (100 μM free calcium), 25 mM TRIS, 1 mM EGTA, and 0.2 mM DTT at pH 7.0 (HCl). The activating solution had the same composition as the nonactivating one plus ATP at a saturating concentration of 100 μM. Solid curve is the best fit of the experimental curve to the biexponential function $A_1\exp(-t/\tau_1) + A_2\exp(-t/\tau_2)$ upon setting $t = 0$ at t_{peak}. Inset shows the plot of I_{peak} (normalized, see text) versus. c_{peak} for various ATP concentrations; the solid curve is the best fit to the Michaelis-Menten equation.

The current starts rising as soon as the first portion of the ATP-containing solution reaches the SSM surface. During the rising portion of the current transient, the ATP concentration in contact with the SSM increases, but its value, c_{peak}, at the current peak is still less than its full value, c_0. The concentration c_{peak} is approximately expressed by the equation

$$c_{peak} = c_0[t_{peak}/(t_{peak} + \tau_{app})], \quad (1)$$

where t_{peak} is the time of the current peak, as measured from the onset of the current rise, and τ_{app} is an empirical parameter, which can be determined as described in Pintschovius and Fendler (1999), provided the ATP dependence of the peak current, I_{peak}, satisfies the Michaelis-Menten equation. (Note that the above authors measure the time from the instant of the electrical signal that activates the electrical valve.) In this case, the best fit of the experimental data was obtained for $\tau_{app} = 92$ ms and for a half-saturating concentration $K_M = 2.9$ μM. The confidence interval for τ_{app} was between 85 and 97 ms. The inset of Fig. 1 shows the experimental plot of I_{peak} versus c_{peak} for various ATP concentrations, c_0; the solid curve is the best fit to the Michaelis-Menten equation. The experimental points were obtained from two sets of current transients recorded on two different SSMs. The error bars express the average standard deviations in the 4–5 repeated measurements routinely carried out on the same SSM. Since the amount of adsorbed vesicles varies from a SSM to another, the peak currents of each set were normalized to their maximum value recorded under ATP saturating conditions, taken as unity. For a detailed analysis, the descending portion of the current transients was fitted with the biexponential function $A_1\exp(-t/\tau_1) + A_2\exp(-t/\tau_2)$, upon setting $t = 0$ at t_{peak} (*solid curve* in Fig. 1). Fig. 2 shows plots of τ_1^{-1} and A_1 versus c_{peak}, as obtained from a single set of current transients. It is apparent that τ_1^{-1}, A_1, and I_{peak} exhibit approximately the same dependence upon the ATP concentration. The second relaxation time constant, τ_2, is practically independent of c_{peak} (data not shown), and amounts to $\sim$300 ms, whereas its amplitude A_2 is positive and more than one order of magnitude smaller than the maximum absolute value of A_1. The second exponential function accounts for the current overshoot, which is evident in the current transient of Fig. 1. The charge under any of the current transients recorded on the same SSM is practically the same for all ATP concentrations, and corresponds to the overall amount of Ca^{2+} ions translocated by the pumps in a cycle. No stationary current is observed, due to the high resistance of the supporting alkanethiol/phospholipid mixed bilayer (see the Appendix).

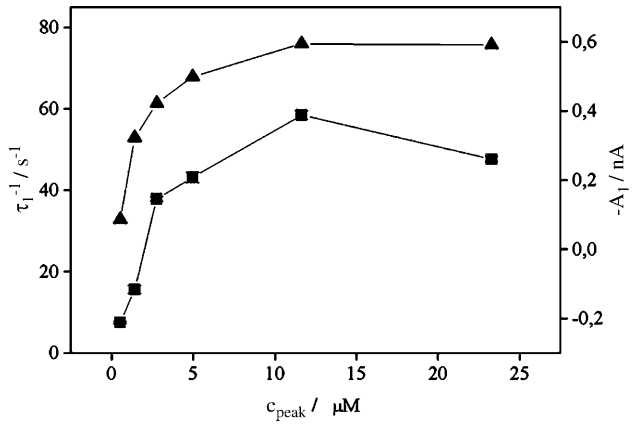

FIGURE 2 Plot of the first relaxation time constant, τ_1 (■), and of the corresponding amplitude, A_1 (▲), versus the corrected ATP concentrations, c_{peak}, under the same conditions as in Fig. 1.

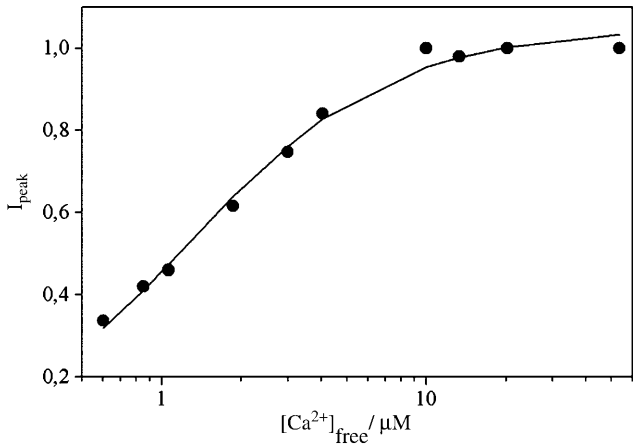

FIGURE 3 Ca^{2+} dependence of 100 μM ATP concentration-jump experiments. The solution contained 150 mM choline chloride, 1 mM $MgCl_2$, 25 mM TRIS, 1 mM EGTA, and 0.2 mM DTT at pH = 7.0 (HCl), and free calcium concentrations ranging from 0.6 to 53.7 μM; the latter were realized by suitable additions of $CaCl_2$. Solid curve is the best fit to Eq. 2.

Inhibition experiments were carried out by first recording a current transient under the same conditions as in Fig. 1, by then adding 0.6 μM thapsigargin directly in the cuvette and by carrying out a further ATP concentration jump after an incubation period of 10 min; the current transient was found to be practically suppressed.

100 μM ATP concentration jumps at different Ca^{2+} concentrations

If jumps of a saturating ATP concentration of 100 μM are carried out in the presence of various Ca^{2+} concentrations both in the nonactivating and in the activating solution, the resulting peak currents depend upon the Ca^{2+} concentration as shown in the semilogarithmic plot of Fig. 3. No correction of the concentration values was required in this mode of concentration-dependent measurement. In fact, even if the ATP concentration in contact with the SSM at the current peak is lower than its full value in view of Eq. 1, it is still high enough to assure saturation of the calcium pumps with the cytoplasmic side facing the aqueous solution.

The experimental points were fitted with the generalized stepwise binding isotherm for two sites (Deranleau, 1969):

$$I = I_{max}\frac{(1/R)Z + Z^2}{1 + (2/R)Z + Z^2}, \quad \text{with } Z \equiv \frac{[Ca^{2+}]}{K_{1/2}};$$
$$K_{1/2} \equiv \frac{1}{\sqrt{K_1 K_2}}; \quad R \equiv 2\sqrt{\frac{K_2}{K_1}}. \qquad (2)$$

Here, Z is the ratio of the free calcium concentration to its experimental half-saturating value, $K_{1/2} = 1.26 \pm 0.08$ μM, whereas K_1 and K_2 are the binding constants for the first and second Ca^{2+} ion. The parameter R measures any cooperativity between the two ions. When R equals unity, the two ions bind independently from each other, and the binding isotherm reduces to a Langmuir isotherm. In this case, K_1 equals $4K_2$, because there are four possibilities for any of the two binding sites being occupied by any of the two still unbound Ca^{2+} ions. Once one of the two binding sites is occupied by one of the two Ca^{2+} ions, the remaining Ca^{2+} ion is left with only one possibility. The best fit to the experimental points in Fig. 3 was obtained for $R = 1.3 \pm 0.3$. The R value being greater than unity denotes a cooperative binding, in qualitative agreement with the literature. The two binding constants K_1 and K_2, derived from Eq. 2 for $K_{1/2} = 1.26$ μM and $R = 1.3$, amount to 1.2×10^6 M^{-1} and 5.1×10^5 M^{-1}, respectively.

Ca^{2+} concentration jumps in the absence of ATP

In Fig. 4, the current transient after a saturating Ca^{2+} concentration jump ($[Ca^{2+}]_{free} = 28.2$ μM) in the absence of ATP (*curve a*) is compared with that after a 100 μM ATP concentration jump in the presence of the same Ca^{2+} concentration, under otherwise identical conditions (*curve b*). The charge under the first current transient, due to Ca^{2+} binding to the pump, is less than the charge under the second transient, due to the ATP-induced Ca^{2+} translocation, by a factor of 0.63. Here and in the following, the charge under the current transients was calculated upon eliminating the contribution from the current overshoot. To this end, the whole charge enclosed between the current transient and the time axis was first measured, including its positive contribution due to the current overshoot. The time axis was taken as the horizontal axis passing by the background current attained toward the end of the 1 s period of exposition of the SSM to the activating solution. This

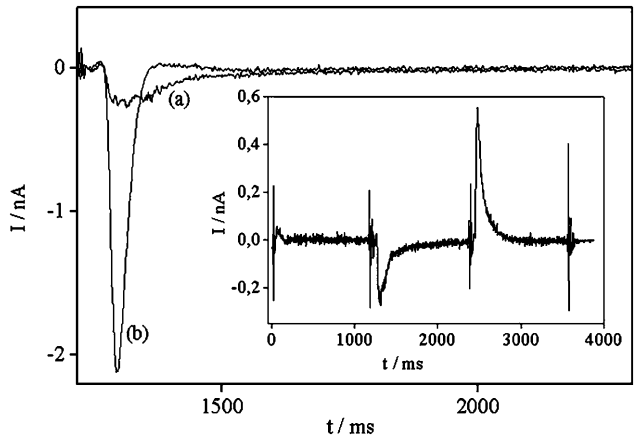

FIGURE 4 Current transients after a 28.2 μM free Ca^{2+} concentration jump in the absence of ATP (*a*) and a 100 μM ATP concentration jump in the presence of 28.2 μM free Ca^{2+} in both the activating and the nonactivating solution (*b*). The nonactivating solution contained 150 mM choline chloride, 1 mM $MgCl_2$, 25 mM TRIS, 0.2 mM EGTA, and 0.2 mM DTT at pH 7.0 (HCl); in the case of curve *b*, it also contained 28.2 μM free Ca^{2+}. Inset shows the on-current after the Ca^{2+} concentration jump in the absence of ATP, as well as the subsequent off-current after the rapid displacement of the Ca^{2+}-containing solution by the nonactivating solution.

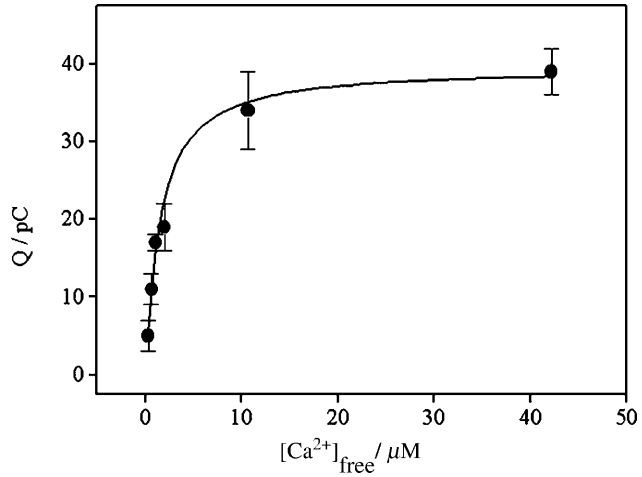

FIGURE 5 Plot of the charge under the off-current transients after Ca^{2+} concentration jumps against the free calcium concentration. The nonactivating solution was the same as in Fig. 4. The free calcium concentration in the activating solution was varied from 0.317 to 42.2 μM by varying the total calcium concentration from 82.5 μM to 0.24 mM. Solid curve is the best fit of the experimental points to the phenomenological Hill function.

overall negative charge was then increased by the negative quantity $A_2\tau_2$, where τ_2 is the relaxation time for the overshoot and A_2 is the corresponding positive amplitude. (See the Discussion section for a justification of this procedure.) For the small $A_2\tau_2$ values normally observed, practically identical results were obtained by measuring only the charge on the negative side of the current axis. Henceforth, the current after the rapid injection of an activating solution into the cuvette will be referred to as the on-current, whereas the current after the subsequent rapid injection of a nonactivating solution will be referred to as the off-current. Clearly, the currents so far described are on-currents.

The inset of Fig. 4 shows the on-current after the Ca^{2+} concentration jump in the absence of ATP, as well as the subsequent off-current after the rapid removal of the Ca^{2+}-containing solution by a solution differing exclusively by the absence of Ca^{2+}; the EGTA contained in this Ca^{2+}-free nonactivating solution was sufficient to remove almost instantaneously the Ca^{2+} ions taken up by the enzyme from the preceding activating solution.

As expected, the charge under the on-current transient was found to be equal and opposite to that under the corresponding off-current transient at all Ca^{2+} concentrations. In fact, whereas the first transient is due to Ca^{2+} binding to the pump, the second one is due to its removal. Fig. 5 shows a plot of the charge under the off-current transient versus the free calcium concentration present in the preceding activating solution. The fit of the experimental points with the Hill function yields a half-saturating Ca^{2+} concentration of 1.5 $\pm$ 0.3 μM and a Hill coefficient of 1.1 $\pm$ 0.2.

The on-current transients were somewhat noisy and of irregular shape at all Ca^{2+} concentrations, often exhibiting a rounded maximum. Conversely, the off-current transients could be satisfactorily fitted with a biexponential model function, $A_{off,1}\ \exp(-t/\tau_{off,1}) + A_{off,2}\ \exp(-t/\tau_{off,2})$. The dependence of the two relaxation time constants, $\tau_{off,1}$ and $\tau_{off,2}$, upon the Ca^{2+} concentration is shown in Fig. 6. At the lowest Ca^{2+} concentrations investigated, the A_1/A_2 ratio is > 20, but then decreases rapidly assuming a value of ~ 2 at Ca^{2+} concentrations ≥ 5 μM.

Inhibition experiments were carried out by first recording a current transient under the same conditions as in curve *a* of Fig. 4, by then adding 0.6 μM thapsigargin directly in the cuvette and by carrying out a further Ca^{2+} concentration

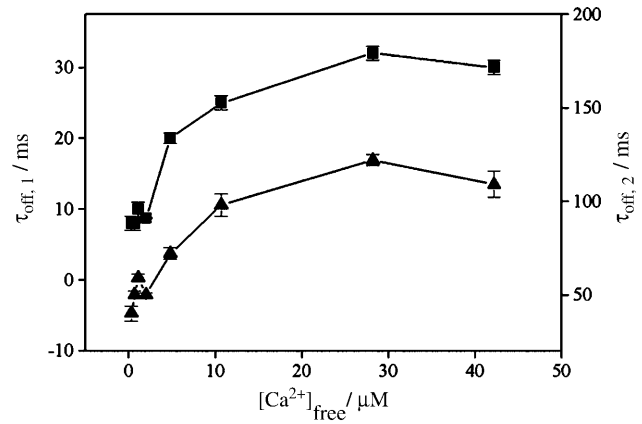

FIGURE 6 Dependence of $\tau_{off,1}$ (■) and $\tau_{off,2}$ (▲) on the free calcium concentration. $\tau_{off,1}$ and $\tau_{off,2}$ are the relaxation time constants of the off-current transients obtained under the same experimental conditions as in Fig. 5.

jump after an incubation period of 10 min; the current transient was found to be practically suppressed.

pH dependence of charge translocation at a constant, saturating Ca^{2+} concentration

Fig. 7 shows a series of current transients after 100 μM ATP concentration jumps in the presence of a free calcium concentration of 100 μM and at different pH values. In this experiment both the calcium ionophore A23187 and the protonophore 1799 were used, to prevent the formation of Ca^{2+} and H^+ gradients across the membrane and to reduce the transmembrane potential. The presence of these two ionophores determined the attainment of a stable stationary ''pump'' current, which was revealed by an appreciable capacitive off-current flowing from the electrode toward the solution, namely in the opposite direction with respect to the on-current. It should be noted that a nonzero stationary pump current does not necessarily involve the flow of a nonzero stationary ''on-current'' along the external circuit. In fact, due to the high resistance of the supporting alkanethiol/phospholipid mixed bilayer, the current transients in Fig. 7 do not show a detectable stationary on-current.

The inset of Fig. 7 shows a plot of the normalized charge Q_N under the on-current transient versus pH, whereas Fig. 8 shows the peak current, I_{off}, and the single relaxation time constant, τ_{off}, of the off-current. The translocated charge Q is practically pH independent over the pH range from 6.5 to 7.0, thus excluding a competition of protons for the Ca^{2+} binding sites over this narrow pH range. A further pH increase from 7 to 8.2 causes Q to grow, tending to a limiting value that is practically twice that at pH < 7. This indicates in a clear and direct way that the effect of protons at physiological pH is that of halving the charge translocated by

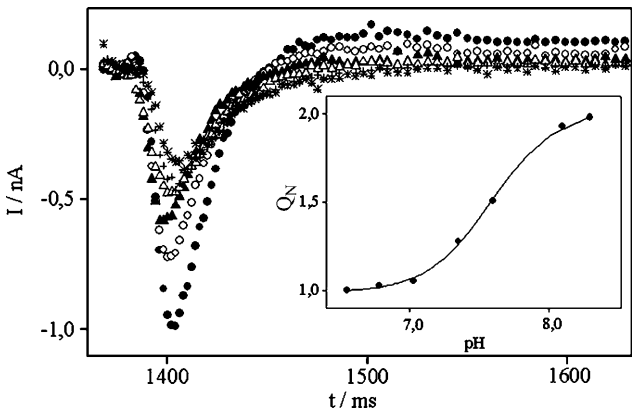

FIGURE 7 Current transients after 100 μM ATP concentration jumps at different pH values: 6.55 (*), 6.78 (+), 7.03 (△), 7.35 (▲), 7.58 (○), and 8.13 (●). The nonactivating and activating solutions had the same composition as in Fig. 1. Both the calcium ionophore A23187 and the protonophore 1799 (1.25 μM) were used. Inset shows the dependence of the normalized charge Q_N under the peaks upon pH. Solid curve is the best fit of the experimental points to the phenomenological Hill function.

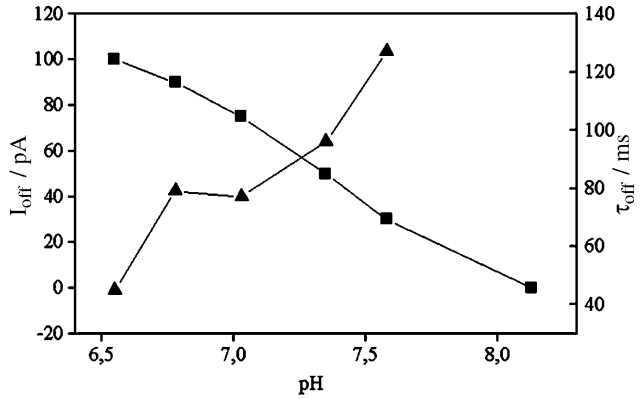

FIGURE 8 Plots of the peak current, I_{off} (■), and of the single relaxation time constant, τ_{off} (▲), of the off-current transients against pH. Data were obtained from the set of current transients in Fig. 7.

the calcium ions, thus supporting the countertransport of one H^+ per one Ca^{2+} reported by Yu et al. (1993). The Q versus pH plot in the inset of Fig. 7 can be fitted with a Hill function, yielding a half-saturating pH value of 7.6 and a Hill coefficient of 1.85 ± 0.2. The Hill coefficient being definitely greater than unity points to a cooperative binding. No attempt was made to use the more general expression of Eq. 2 for the fitting; in fact, in this case the Hill coefficient is so close to 2 that the R value resulting from such a fitting is very high, and consequently its accuracy is very low.

Influence of K^+ on charge translocation

In the above concentration-jump experiments, potassium ion was absent, even though it is present at a concentration of 160–175 mM in the cytoplasmic space of muscle (Sreter, 1963). To determine its influence on Ca^{2+} translocation, 100 μM ATP concentration jumps were carried out in the presence of a saturating 28 μM free calcium concentration and of increasing amounts of K^+. The ionic strength of the solution during the concentration jumps was kept constant by increasing the concentration of KCl at the expense of that of choline chloride. Fig. 9 shows the resulting current transients at different K^+ concentrations. The inset of Fig. 9 shows the normalized peak current as a function of the K^+ concentration. It is apparent that potassium ion decreases the peak current up to reducing it to ~½. This decrease can be fitted with the function

$$I = I_0 - \frac{(I_0 - I_{min})}{1 + K_{decay}/[K^+]}, \quad (3)$$

yielding a K_{decay} value of 18 ± 4 mM. For $[K^+] \leq 100$ mM, the charge under the current transient decreases with increasing $[K^+]$, in the same way as the peak current does; moreover, the decreasing branch of the current transient can be satisfactorily fitted by a single exponential function, with a relaxation time constant of 15 ms. These results agree with

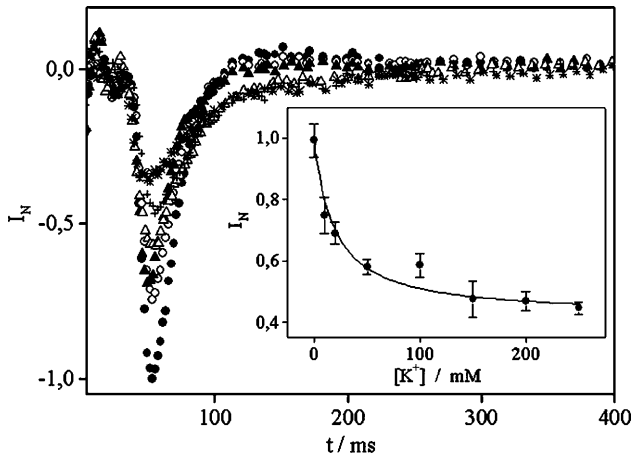

FIGURE 9 Current transients after 100 μM ATP concentration jumps in the presence of different K^+ concentrations: 0 (●), 10 (○), 20 (▲), 100 (△), 200 (+), and 225 (*) mM. Currents were normalized to the maximum peak current, taken as unity. The nonactivating solution contained x mM KCl, with $0 < x < 225$ mM, $(250 - x)$ mM choline chloride, 1 mM $MgCl_2$, 0.225 mM $CaCl_2$ (28 μM free calcium concentration), 25 mM TRIS, 0.2 mM EGTA, and 0.2 mM DTT at pH 7.0 (HCl). The activating solution had the same composition as the nonactivating one plus 100 μM ATP. Inset shows the dependence of the normalized peak current on the K^+ concentration. Solid curve is the best fit of the experimental points to Eq. 3.

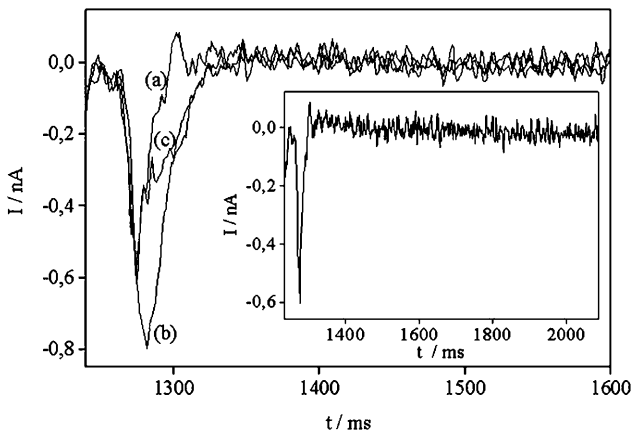

FIGURE 10 Current transients after a 30 mM KCl concentration jump (*a*), a 100 μM ATP concentration jump (*b*), and a simultaneous 30 mM KCl and 100 μM ATP concentration jump (*c*), all in the presence of calcium ions. In all experiments, the same nonactivating solution was used, which contained 250 mM choline chloride, 1 mM $MgCl_2$, 0.225 mM $CaCl_2$, 25 mM TRIS, 0.2 mM EGTA, and 0.2 mM DTT at pH 7.0 (HCl). In experiment *a*, the activating solution contained 30 mM KCl, 220 mM choline chloride, and the remaining components as in the nonactivating solution; in experiment *b*, the activating solution had the same composition as the nonactivating solution plus 100 μM ATP; in experiment *c*, the activating solution differed from that of experiment *a* by the presence of 100 μM ATP. Inset shows the sole curve *a*.

those of Hartung et al. (1997), who observed that the presence of 50 mM K^+ causes the amplitude of the current transient after an ATP concentration jump on SR fragments adsorbed on a BLM to be reduced by ~50%, whereas the time course is nearly unchanged. From Fig. 9 it is apparent that for $[K^+] > 100$ mM, the current transients show a tail than lasts for almost 40 ms.

A 30 mM K^+, concentration jump in the absence of ATP and Ca^{2+} yields a negative current transient that decays in time very rapidly, with a relaxation time constant of ~10 ms. The negative sign of the current denotes a flow of positive charge from the solution toward the SSM, pointing to an electrogenic K^+ binding to the calcium pump (*inset* of Fig. 10). This current transient remains substantially unaltered in the presence of a saturating 100 μM free calcium concentration (data not shown). The charge under the current transient after the 30 mM K^+ concentration jump is ~40% of that after an ATP concentration jump on the same SSM in the presence of a saturating free calcium concentration and in the absence of K^+ (compare *curves a* and *b* in Fig. 10). Curve *c* in Fig. 10 is the current transient after a concentration jump of both 100 μM ATP and 30 mM K^+, still on the same SSM. It is evident that the first portion of curve *c* is due to the rapid binding of K^+ ions to the pump. This is followed by the current due to the Ca^{2+} translocation induced by ATP, which is clearly smaller than the same current in the absence of K^+ (*curve b*), although it ultimately merges with the latter and decays in time with the same relaxation time constant. To verify the possible effect of any K^+ channels present in the SR vesicles upon the above K^+ concentration jumps, the following control measurements were performed. After carrying out a 25 mM K^+ concentration jump in the absence of Ca^{2+}, the same jump was repeated in the presence of 100 μM TEA chloride, which is known to block K^+ channels. Fig. 11 shows that the presence of TEA causes the charge under the current transient to decrease by only ~20% (see also the *inset* of Fig. 11). Upon removing TEA from the solution and carrying out a further K^+ concentration jump, the original current transient was recovered. The SR vesicles adsorbed on the SSM were then incubated with 0.6 μM thapsigargin for 10 min and a further K^+ concentration jump was carried out. The charge under the resulting current transient was found to decrease by ~90% (see the *inset* of Fig. 11). This indicates that the current transient after a K^+ concentration jump is mainly to be ascribed to Ca-ATPase.

DISCUSSION

Upon addition of ATP to Ca-ATPase preincubated with Ca^{2+}, a capacitive current with a rapid rise and a slower decay was observed, within the time-frame of a single catalytic cycle. The kinetics and extent of the current were found to depend on the ATP and Ca^{2+} concentrations. The current is to be ascribed to an electrogenic phenomenon, related to Ca^{2+} translocation. The magnitude of the current is reduced by lowering the pH, indicating that the electrogenic phenomenon is counteracted by protons.

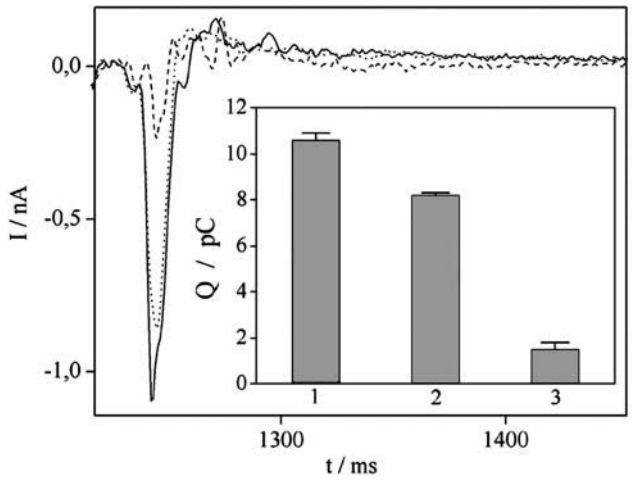

FIGURE 11 Current transients after 25 mM K^+ concentration jumps. Solid curve was obtained with an activating solution containing 25 mM KCl, 125 mM choline chloride, 1 mM $MgCl_2$, 25 mM TRIS, 0.25 mM EGTA, and 0.2 mM DTT at pH 7.0 (HCl), and with a nonactivating solution differing from the activating one by the replacement of 25 mM KCl with 25 mM choline chloride. Dotted curve was obtained under the same conditions as the solid one, apart from the addition of 100 μM TEA chloride to both the activating and the nonactivating solution. Dashed curve was obtained under the same conditions as the solid curve, apart from the addition of 0.6 μM thapsigargin in the cuvette and an incubation period of 10 min before the K^+ concentration jump. Inset shows the charge under the solid (*1*), dotted (*2*), and dashed curve (*3*). Error bars express the average standard deviations in the four repeated measurements carried out on the same SSM.

ATP concentration jumps

The current transients due to ATP concentration jumps, such as that in Fig. 1, can be fitted with a biexponential function, yielding an ATP-dependent relaxation time constant τ_1 and an ATP-independent one, $\tau_2 \cong 300$ ms. By performing ATP concentration jumps on fragmented SR adsorbed on a BLM, via the light-induced conversion of caged ATP, Hartung et al. (1997) fitted the resulting current transients with a sum of four exponential functions. The first two relaxation time constants are $\leq$5 ms and, therefore, cannot be observed with the technique in this study, because they are shorter than t_{peak}. The values of the ATP-dependent time constant, denoted by τ_3 by the authors, were found to depend somewhat on whether the concentration of the photo-released ATP was changed by varying the caged ATP concentration at constant flash energy or by varying the latter at constant concentration of caged ATP. Values of τ_3^{-1} at saturating ATP were reported to range from 35 to 100 s^{-1}, depending on the experimental conditions. These values are in fairly good agreement with the τ_1^{-1} value of $\sim$50 s^{-1} reported in Fig. 2. The dependence of the time constant τ_3 upon the ATP concentration was described by a Michaelis-Menten formalism with a half-saturating concentration $K_M = 4.6$ μM (Hartung et al., 1997), which is close to the value, 2.9 μM, obtained from the fit in the inset of Fig. 1. In view of its dependence on ATP concentration, the relaxation time constant at hand must be related to the binding of ATP to Ca-ATPase. The fourth time constant, τ_4, reported by Hartung et al. (1997) is independent of the ATP concentration, is associated with a positive amplitude, and amounts to $\sim$330 ms. This time constant accounts for a moderate current overshoot and is entirely analogous to the time constant τ_2 reported herein. These authors tentatively ascribe it to the proton countertransport after Ca^{2+} translocation. In principle, however, the overshoot may also be ascribed to the response of the system, consisting of the supporting mixed bilayer and of the adsorbed vesicles, to the pumping of Ca-ATPase, as discussed below.

It is useful to consider our observations in the light of the Ca^{2+}-ATPase reaction sequence and a minimal number of partial reactions as outlined in Fig. 12. From the initial linear section of the τ_1^{-1} versus c_{peak} plot in Fig. 2, a rate constant, k_1, of $\sim 1.2 \times 10^7$ $M^{-1}s^{-1}$ is obtained. In view of its dependence on ATP concentration, this rate constant must be related, either directly or indirectly, to the binding of ATP to the enzyme. Butscher et al. (1999) reported that phosphorylation and conformational transitions of Ca-ATPase exhibit only minor electrogenicity. It is, therefore, reasonable to conclude that k_1 is to be ascribed to a step after a diffusion-limited ATP binding step in quasi-equilibrium. With this assumption, k_1 is the product of the rate constant for the rate-limiting step and the equilibrium constant for the preceding ATP binding step. Considering an equilibrium constant of 3×10^5 M^{-1} for ATP binding (Fig. 1), and $\sim 10^2$ s^{-1} rate constant for the steps related to enzyme phosphorylation and release of bound Ca^{2+} (Inesi et al., 1988), the resulting product is 3×10^7 $M^{-1}s^{-1}$, in close agreement with the k_1 value obtained in our experiment. It is then apparent that the electrogenicity of the pump is related to lumenal release of Ca^{2+} after enzyme phosphorylation by ATP, as expected.

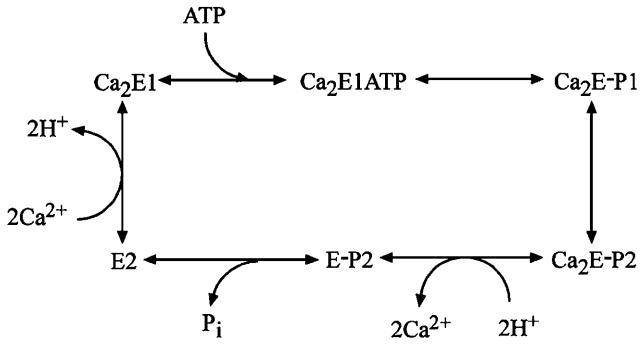

FIGURE 12 Simplified catalytic and transport cycle for the Ca^{2+}-ATPase. Each ATPase molecule has two Ca^{2+} binding sites and one catalytic site. Phosphorylated enzyme intermediate (E-P) is formed by utilization of ATP, after activation by Ca^{2+}. Interconverting states of the protein display high affinity and cytosolic orientation (E_1 and E_1-P), or low affinity and lumenal orientation (E_2 and E_2-P) of the Ca^{2+} sites. In the forward direction of the cycle, the phosphorylation potential of ATP is utilized to reduce the affinity of the Ca^{2+} sites. At neutral pH, two Ca^{2+} are exchanged with two H^+. Kinetic and equilibrium constants for the partial reactions were previously characterized in detail (Inesi et al., 1988).

Contributions to the on- and off-current transients

The system consisting of the supporting mixed bilayer and of the adsorbed vesicles can be represented by the equivalent circuit of Fig. 13 (Dolfi et al., 2002), which differs from that adopted by Bamberg et al. (1979), Borlinghaus et al. (1987), and Fendler et al.(1993) only by the presence of the external applied potential E. Here, the calcium pump is represented as a current source, and the dependence of the pump current, I_p, on time is expressed a priori as a sum of exponentially decaying contributions plus a constant contribution b, which represents the stationary pump current (Borlinghaus et al.,1987):

$$I_p(t) = \sum_{i=1}^{n} a_i \exp(-t/\tau_i) + b. \quad (4)$$

The SR vesicle is represented as a current source (the Ca-ATPase), in parallel with the resistance R_p and the capacitance C_p of the vesicle. The mixed bilayer supporting the SR vesicle is represented as a further R_mC_m mesh in series with the vesicle. The equivalent circuit is closed on the external applied potential E. The current source is activated at time $t = 0$ and deactivated at time $t = T$ by a gate function, $G(t,T)$, namely a function representing a rectangular pulse of unit height that starts at $t = 0$ and lasts for a time T. The analysis of this equivalent circuit, briefly outlined in the Appendix, yields Eqs. A2 and A3 for the on- and off-current. The on-current of Eq. A2 consists of two constant contributions and of a number of exponential functions. In addition to the exponential functions with the time constants τ_i of the pump current of Eq. 4, a further exponential function is present, whose time constant, $\tau_c=(C_p + C_m)R_mR_p/(R_m + R_p)$, depends exclusively on the resistive and capacitive elements of the equivalent circuit. The resistance R_m and capacitance C_m of the mixed bilayer, which were directly obtained from impedance spectroscopy measurements in the absence of the SR vesicles, amount to $\sim$7 MΩ cm^2 and 0.2 μF cm^{-2}, whereas the capacitance C_p of the vesicle can be ascribed the reasonable value of 1 μF cm^{-2}. Therefore, the time constant τ_c, when experimentally accessible, may allow an estimate of R_p. In practice, $R_m \gg R_p$, such that τ_c is practically equal to $(C_p + C_m)R_p$. The amplitude of the exponential function of time constant τ_c is practically given by $[C_m/(C_m + C_p)]\{\Sigma_i[a_i\tau_i/(\tau_c - \tau_i)]-b\}$, since $\tau_m \gg \tau_c$. If, as is often the case, $\tau_c > \tau_i$ for all the exponentially decaying contributions to the current, then the above amplitude is positive, yielding a current overshoot, provided that $\Sigma_i[a_i\tau_i/(\tau_c - \tau_i)] > b$. The reason for the overshoot is as follows: As soon as the pump is activated, the pump current flows along the R_p and C_p branches in the direction of the arrows in Fig. 13. Under these conditions, the capacitive coupling with the R_mC_m mesh causes the experimental on-current, I_{on}, to flow along the external circuit in the direction from the solution to the SSM. This is due to the potentiostatic system, which keeps the potential difference across the whole metal/solution interface constant. Consequently, the potential difference across the vesicular membrane (positive toward the metal) built up by the pumping of Ca^{2+} ions is instantaneously compensated for by an equal and opposite potential difference across the mixed thiol/lipid bilayer, which is built up by a flow of electrons along the external circuit toward the metal surface; this corresponds to a negative capacitive current from the electrode toward the solution. This negative capacitive current is expressed by the first term between square brackets in Eq. A2, which is practically given by $-[C_m/(C_m + C_p)][\Sigma_i a_i \exp(-t/\tau_i)]$, when τ_m and τ_c are both much greater than any of the relaxation times τ_i of the pump, as is often the case. This indicates that the capacitive coupling decreases the exponential decaying contributions to the pump current by a factor $[C_m/(C_m + C_p)]$. After this initial flow of negative current, if the pump current decays vary rapidly, the capacitance C_p may tend to be discharged across R_p, causing a decrease in the potential difference across C_p, with a resulting inversion of the I_{on} capacitive current (i.e., the overshoot). As appears from the expression for the amplitude of the exponential function of time constant τ_c, the overshoot is expected to decrease with an increase of the stationary pump current b, up to being completely suppressed. In fact, a sufficiently high b value prevents the capacitance C_p from being discharged during the activation period, $0 < t < T$, of the pump. Rather, the capacitance C_p remains charged until the pump is inactivated by the solution flux that removes the activating substance from the contact with the SSM, at time $t = T$. As soon as the pump is inactivated, C_p is discharged causing a positive capacitive I_{off} current. Eq. A4 shows that, under usual experimental conditions, I_{off} decays with the time constant τ_c (see the Appendix). Thus, if on the one hand a finite stationary pump current b decreases, or even suppresses, the overshoot, on the other hand it determines a finite off-current, whose relaxation time constant τ_c may still allow an estimate of R_p, whereas the corresponding amplitude allows an estimate of b (see later). It is evident that, to estimate the exponentially decaying contributions to the pump current $I_p(t)$ multiplied by the $[C_m/(C_m + C_p)]$

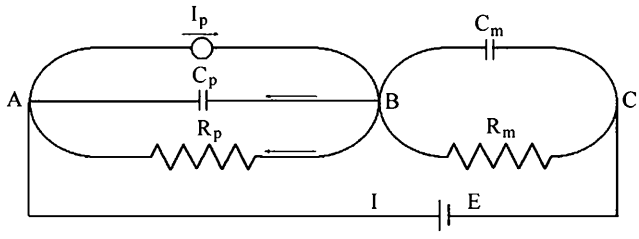

FIGURE 13 Equivalent circuit simulating the mixed bilayer and the SR vesicles adsorbed on it. I_p is the pump current, I the current flowing along the external circuit, and E the external applied potential. C_p and R_p are the capacitance and resistance of the vesicles, and C_m and R_m those of the mixed bilayer.

factor, the positive term decaying with the relaxation time τ_c in the expression of Eq. A2 for the overall negative on-current must be subtracted from this current, thus increasing the absolute value of the resulting negative on-current. The contribution from the overshoot to the charge under the on-current transient is clearly given by the product of its relaxation time τ_c by the corresponding amplitude.

Equations A2 and A3 show that both I_{on} and I_{off} are characterized by a time-independent contribution, $-E/(R_m + R_p)$, which flows along the external circuit during both the activating and inactivating periods. In practice, however, the resistance R_m is so high that this contribution is vanishingly small. This implies that, by our procedure, the potential difference across the vesicular membrane cannot be affected by varying the applied potential E, because any change in E tends to be located across the mixed thiol/lipid bilayer. Equation A2 also shows that, in principle, a finite stationary pump current b generates a stationary contribution to the experimental I_{on} current; this is given by $-[C_m/(C_m + C_p)]b(\tau_c/\tau_m)$, with $\tau_m \equiv R_m C_m \cong 1.4$ s. In practice, however, $\tau_m \gg \tau_c$, so that the above capacitive coupling eliminates completely the stationary contribution to I_{on}.

The equivalent circuit adopted herein and represented in Fig. 13 appears to be more realistic for adsorbed flat membrane fragments incorporating integral proteins than for adsorbed proteoliposomes. However, the current is only pumped on the free membrane area, A_f, of the adsorbed vesicles. If we denote by A_c the area of the vesicle-covered surface of the supporting mixed bilayer, approximately identified with the contact area of the vesicles, it can be shown that the experimental on-current, suitably corrected for any current overshoot, is approximately given by $I(t) = -\{C_m/[C_m(1 + \rho) + \rho\, C_p]\}I_p(t)$, with $\rho = A_f/A_c$ (Läuger, 1991). Therefore, the interpretation of experiments with adsorbed membrane sheets and adsorbed vesicles is similar, the only difference being the magnitude of the scaling factor relating $I(t)$ and $I_p(t)$.

Hartung's tentative justification for the overshoot by proton countertransport is disproved by the pH dependence of the current transients due to the ATP-induced Ca^{2+} translocation (see Fig. 7). Thus, the overshoot is more pronounced at pH 8.13, when proton translocation is practically suppressed (see below). Conversely, the explanation of the overshoot by the exponential term of time constant τ_c in Eq. A2 is supported by the observation that it increases in parallel with a decrease in the amplitude of the off-current (see Fig. 8); Eq. A4 shows that such a decrease is due to a decrease in b, which is expected to determine an increase in the overshoot.

Ca^{2+} concentration jumps in the absence of ATP

The Ca^{2+} dependence of the current transient after a saturating ATP concentration jump is characterized by a half-saturating Ca^{2+} concentration $K_{1/2} = 1.26 \pm 0.08$ μM, and by binding constants for the first and second Ca^{2+} ion about equal to $K_1 = 1.2 \times 10^6\ M^{-1}$ and $K_2 = 5.1 \times 10^5\ M^{-1}$; these two values denote a moderate cooperativity in the binding. The $K_{1/2}$ value is in good agreement with that of 1 μM (range 0.5–1.2 μM), obtained by Hartung et al. (1987) from SR vesicles adsorbed on a BLM. This value is in reasonable agreement with the concentration dependence of the rate of ATP hydrolysis, which is half-maximal at 0.1–0.2 μM Ca^{2+} (Hartung et al., 1987, and references therein).

The current transient after an ATP concentration jump and the charge after a Ca^{2+} concentration jump in the absence of ATP exhibit a very similar dependence upon the Ca^{2+} concentration (compare Figs. 3 and 5). Thus, the half-saturating Ca^{2+} concentration amounts to 1.26 ± 0.08 μM in the first case and to 1.5 ± 0.3 μM in the second. Moreover, both dependencies point to a slight cooperativity in the binding of the two Ca^{2+} ions (an R value of 1.3 in the first case, a Hill coefficient of 1.1 in the second). This result is to be expected, since the magnitude of the current transient after an ATP concentration jump on SR vesicles preincubated in Ca^{2+} is a measure of the amount of Ca^{2+} bound to the pump before its activation. The Ca^{2+} dependence in Fig. 5 is in good agreement with the Ca^{2+} dependence of the increase in tryptophan fluorescence intensity induced by Ca^{2+} binding to Ca-ATPase in the absence of ATP. Thus, the half-saturating Ca^{2+} concentration, $K_{1/2}$, in the presence of 1 mM Mg^{2+} amounts to 1.4 μM (see Fig. 6 in Henderson et al., 1994). Somewhat lower values of $K_{1/2}$ at pH 6.8–7.4 were reported by Inesi et al. (1980) (0.5 μM) and by Peinelt and Apell (2002) (0.59 μM); moreover, in both cases a Hill coefficient close to 2 was reported, thus suggesting a strong cooperativity in the binding of the two Ca^{2+} ions. The discrepancy between the above high cooperativity and the apparently slight cooperativity found herein can be possibly explained if the binding of the second Ca^{2+} ion to be bound or the release of the second Ca^{2+} ion to be released do not reach full equilibrium conditions during the presteady-state measurements in this study. In fact, a high cooperativity implies that the binding of the second Ca^{2+} ion to be bound, or the release of the second Ca^{2+} ion to be released, is favored with respect to the case that the two binding sites are occupied independently. In this respect it should be noted that strong evidence exists that the binding of the second Ca^{2+} ion is preceded by a conformational change induced by the binding of the first Ca^{2+} ion (Inesi et al., 1980; Henderson et al., 1994), according to the following mechanism:

$$E_1 + Ca^{2+} \overset{1}{\leftrightarrow} E_1Ca \overset{3}{\leftrightarrow} E_1^*Ca + Ca^{2+} \overset{2}{\leftrightarrow} E_1^*Ca_2. \quad (5)$$

Since the phenomenological Hill function ignores the presence of conformational transitions between successive ion binding steps, a Hill coefficient close to unity does not exclude a strong cooperativity. Thus, in the case of the

mechanism of Eq. 5, three equilibrium constants must be introduced:

$$K_1 = \frac{[E_1Ca]}{[E_1][Ca^{2+}]}; \quad K_3 = \frac{[E_1^*Ca]}{[E_1Ca]};$$
$$K_2 = \frac{[E_1^*Ca_2]}{[E_1^*Ca][Ca^{2+}]}. \tag{6}$$

The fractional saturation y, namely the equilibrium average value of Ca^{2+} ions bound per site, is then given by

$$y = \frac{[E_1Ca] + [E_1^*Ca] + 2[E_1^*Ca_2]}{2([E_1] + [E_1Ca] + [E_1^*Ca] + [E_1^*Ca_2])}$$
$$= \frac{(K_1 + K_1K_3)[Ca^{2+}] + 2K_1K_2K_3[Ca^{2+}]^2}{2(1 + (K_1 + K_1K_3)[Ca^{2+}] + K_1K_2K_3[Ca^{2+}]^2)}, \tag{7}$$

where account has been taken that, in principle, each conformation of the pump may provide two binding sites for Ca^{2+}. If $K_3 \ll 1$, it may be readily shown that Eq. 7 reduces to

$$y = \frac{(1/R)Z + Z^2}{1 + (2/R)Z + Z^2} \quad \text{with:} \quad Z \equiv \frac{[Ca^{2+}]}{K_{1/2}};$$
$$K_{1/2} \equiv \frac{1}{\sqrt{K_1K_2K_3}}; \quad R \equiv 2\sqrt{\frac{K_2K_3}{K_1}}. \tag{8}$$

This equation is identical with Eq. 2, apart from the replacement of the second binding constant K_2 by the product K_2K_3. Therefore, even if the second binding site has a higher affinity for Ca^{2+} than the first ($K_2 \gg K_1$), the ''cooperativity parameter'' R may still be close to unity when $K_3 \ll 1$, namely when the conformational equilibrium is shifted toward the E_1Ca form. From Eq. 8 it is also apparent that the Hill function with a Hill coefficient equal to 2 requires that R be $\gg 1$, a situation that may not be satisfied even for $K_2 \gg K_1$, if $K_3 \ll 1$. If, in addition, the equilibrium of the conformational step is not fully attained in the current transients in this study, then the net effect is qualitatively analogous to that of an apparently lower K_3 value, and hence of an apparently weaker cooperativity.

Different views on the conformational transition $E_1Ca \leftrightarrow E_1$*Ca are reported in the literature. Henderson et al. (1994) regard this transition as in quasi-equilibrium, with an equilibrium constant of unity, on the basis of the belief that tryptophan fluorescence intensity is unlikely to be equally sensitive to the occupancy of the two different binding sites by Ca^{2+} ions. On the other hand, Inesi et al. (1980) consider the conformational transition as a slow step (see also Dupont and Leigh, 1978), appreciably shifted toward the E_1Ca form, on the basis of equilibrium binding data combined with electron paramagnetic resonance spectroscopic measurements on spin-labeled preparations sensitive to conformational changes.

Some evidence for cooperativity in the binding of the two Ca^{2+} ions is provided by the time dependence of the off-current after Ca^{2+} concentration jumps in the absence of ATP. This off-current fits to the sum of two exponentials, whose time constants are reported in Fig. 6. When the Ca^{2+} concentration in the activating solution that precedes the jump of the Ca^{2+}-free nonactivating solution is saturating, fast and slow components of the off-current have time constants $\tau_{1,off} \cong 30$ ms and $\tau_{2,off} \cong 120$ ms. This behavior may be consistent with a sequential mechanism in which Ca^{2+} binding occurs in a protein crevice (Inesi, 1987; Inesi et al., 1990), in which the dissociation of the Ca^{2+} ion that is bound first is blocked by the second Ca^{2+} ion that is bound in the same crevice. Under this assumption, the fast component is due to the release of this second Ca^{2+} ion, whereas the slow component is due to the release of the Ca^{2+} that was bound first. A biexponential decrease in tryptophan fluorescence intensity due to Ca^{2+} dissociation induced by an EGTA concentration jump in the presence of Mg^{+2} was reported by Henderson et al. (1994), but the dissociation rate constant for the Ca^{2+} ion released first was considered to be lower than that for the Ca^{2+} ion released second. A biexponential decrease of the intrinsic fluorescence due to Ca^{2+} dissociation from SR vesicles, induced by EGTA in the presence of Mg^{2+}, was also reported by Moutin and Dupont (1991); the corresponding relaxation time constants, 18.5 and 102 ms, are relatively close to those obtained herein.

From Figs. 5 and 6 it is apparent that the two time constants $\tau_{1,off}$ and $\tau_{2,off}$ increase in parallel with the increase in the amount of Ca^{2+} ions bound to the pump. This behavior cannot be explained by assuming bidirectional Ca^{2+}-binding steps in Eq. 5, namely steps in which the backward rate cannot be entirely neglected with respect to the forward one; in fact, the concentration jump of the deactivating solution containing EGTA removes Ca^{2+} ions from the electrode surface. Even upon assuming the presence of residual Ca^{2+} ions in the unstirred layer, the increase in their concentration would cause a decrease in the relaxation time constant, rather than its increase. Thus, in a bidirectional dissociation step $PL \Leftrightarrow P + L$, where P is the pump, L is the ligand, and $([P] + [PL])$ is the constant overall concentration of the pump, the dissociation rate decreases exponentially in time, with a relaxation time constant equal to $(k_f + k_b[L])^{-1}$, where k_f and k_b are the rate constants for the forward and backward process. The experimental increase in the two time constants $\tau_{1,off}$ and $\tau_{2,off}$ with an increase in the amount of bound Ca^{2+} ions can be explained by assuming that a progressive increase in the number of calcium pumps with two bound Ca^{2+} ions causes a slowdown in their release due to cooperativity in their binding.

The dielectric coefficient of the Ca^{2+} binding steps

From Fig. 4 it is apparent that the charge under the on-current transient due to Ca^{2+} binding to Ca-ATPase in the absence

of ATP is less than the charge under the on-current transient due to the ATP-induced Ca^{2+} translocation, as recorded on the same SSM, by a factor of 0.63. To compare these two different charge values, it is first necessary to estimate at which stage of the pump cycle, after its activation by ATP, a stationary pump current is attained. In fact, the capacitive coupling realized by our technique suppresses the measured current as soon as the pump current attains a stationary value (see above). Since the activation of the pump preincubated with Ca^{2+} starts from the E_1*Ca_2 state, it is reasonable to assume that the pump enters the stationary regime immediately after returning to this state. This conclusion is supported by the observation that the charge translocated at pH 7, when full proton countertransport takes place, is practically one-half that translocated at pH 8.2, when proton countertransport is suppressed (see *inset* in Fig. 7). At pH 7, the sum of the dielectric coefficients of all the steps composing a single turnover of the pump equals 2. Incidentally, the dielectric coefficient of a step is the fraction of the thickness of the membrane, assumed to be a homogeneous dielectric film, across which the charge is translocated during the given step times the translocated charge expressed in electronic units. Let x denote the fraction of the membrane thickness, as measured from the cytoplasmic side, at which the Ca^{2+} binding sites are located in the E_1* conformation. Upon assuming that no appreciable movements of charged residues of the pump take place during ion binding and release, the dielectric coefficients relative to the passage from a group of elementary steps to the subsequent one in a cycle is given by

$$E_1^*Ca_2 \overset{4(1-x)}{\longleftrightarrow} P - E_2 \overset{-2(1-x)}{\longleftrightarrow} P - E_2H_2 \overset{-2x}{\longleftrightarrow} E_1 \overset{4x}{\longleftrightarrow} E_1^*Ca_2 \quad (9)$$

in the presence of proton countertransport at pH 7, and by

$$E_1^*Ca_2 \overset{4(1-x)}{\longleftrightarrow} P - E_2 \overset{0}{\longleftrightarrow} E_1 \overset{4x}{\longleftrightarrow} E_1^*Ca_2 \quad (10)$$

in its absence, at pH 8.2. It is readily seen that the only possibility for the charge translocated at pH 8.2 being twice that at pH 7 for any x value is that the stationary pump current starts immediately after the attainment of the next E_1*Ca_2 state. The charges involved in the $E_1 \leftrightarrow E_1$*Ca_2 steps and in a whole enzymatic cycle of the Ca pump at pH 7 amount to 50 and 79 pC on the same SSM. Upon regarding them as proportional to $4x$ and to 2, in view of Eq. 9, an x value of 0.32 is obtained for the fractional distance of the Ca^{2+} binding sites from the cytoplasmic side. This conclusion is in good agreement with the highly resolved three-dimensional structures of the Ca-ATPase of the SR in the E_1 conformation with 2 Ca^{2+} ions bound (Toyoshima et al., 2000) and in the E_2 conformation stabilized by the specific inhibitor thapsigargin (Toyoshima and Nomura, 2002); according to these structures the Ca^{2+} binding moiety is located inside the membrane domain, at ~30–40% of the membrane thickness from the cytoplasmic side.

pH dependence of Ca^{2+} translocation

The curve of the charge Q_N under the on-current transient due to Ca^{2+} translocation against pH can be fitted by a Hill function, with a half-saturating pH value of 7.6 and a Hill coefficient of 1.85 ± 0.2 (see the *inset* of Fig. 7). It should be noted that, whereas a peak current measures the kinetics of a process, the measurement of the charge under the corresponding current transient can be regarded as an equilibrium measurement based on the amount of charge translocated during a single cycle, under presteady-state conditions. The free calcium concentration of 100 μM adopted in these measurements is practically saturating for the initial E_1*Ca_2 state (Butscher et al., 1999; Peinelt and Apell, 2002), and therefore no competition by protons on the cytoplasmic side is to be expected. Hence, the pH dependence of Q_N observed at pH $>$ 7 can be reasonably ascribed to the pH dependence of the P-E_2 conformation on the lumenal side. The half-saturating pH value of 7.6 agrees with that, 7.7, obtained by Yu et al. (1994) from the initial rates of H^+ ejection and Ca^{2+} uptake with reconstituted proteoliposomes upon keeping the cytoplasmic medium at pH 7, where H^+ dissociation is complete, and varying the lumenal pH. The pH dependence of the percentage saturation of H^+ binding obtained by these authors satisfies a Hill equation with a coefficient of 0.9, to be compared with the 1.85 value obtained herein. This difference in Hill coefficients may possibly be ascribed to the different solution composition and/or to the fact that the data by Yu et al. (1994) were obtained from initial rates. An appreciably lower half-saturating pH value of ~5.7 was obtained by Peinelt and Apell (2002) from fluorescence measurements on SR membranes in the presence of ATP, over a broad range of Ca^{2+} concentrations. In this case the Ca-ATPase was under continuous turnover conditions, with a much longer average time spent in the P-E_2 conformation than in the E_1 one. More recently, the same authors (Peinelt and Apell, 2004), on the basis of ATP concentration jump experiments, reported that the two protons bind with a pK of the order of 7.6, in agreement with our results.

The presence of the A23187 ionophore and of the 1799 protonophore induces a stationary pump current, which is revealed by an appreciable off-current, whose time constant, τ_{off}, and peak value, I_{off}, vary with pH as shown in Fig. 8. Noting from Eq. A4 that τ_{off} is given by $\tau_c \approx (C_p + C_m)R_p$, with $C_m = 0.2\ \mu F\ cm^{-2}$ and $C_p \cong 1\ \mu F\ cm^{-2}$, the resistance R_p of the SR membrane in KΩ cm^2 is simply obtained by multiplying the τ_{off} values in Fig. 8 by 0.830. In practice, R_p varies from 37 to 108 KΩ cm^2 as the pH is increased from 6.55 to 7.58. This increase in resistance is ascribed, at least partially, to the decrease in the concentration of protons, which contribute to the conductance of the SR membrane via

the 1799 protonophore. The above R_p values are comparable with those obtained by Hartung et al. (1997) from the decay of the voltage across the SR membrane after cessation of the activity of Ca-ATPase. A similar procedure had previously been adopted by Yu et al. (1993) with reconstituted unilamellar liposomes, obtaining an R_p value of $4 \times 10^7\ \Omega\ cm^2$.

In view of Eq. A4, the peak off-current, I_{off}, is approximately proportional to the stationary pump current b according to the proportionality constant $C_m/(C_m + C_p)$. In this case this constant equals 0.167, and therefore b decays from ~600 pA to zero as pH increases from 6.55 to 8.13 (see Fig. 8). This decrease in b is also confirmed by the on-current overshoot that is clearly visible in the on-current transients of Fig. 7 for pH values >7.5. The latter on-current transients could be fitted with a biexponential function, yielding a time constant of positive amplitude, due to the overshoot, which amounts to ~250 ms. In view of Eq. A4, this time constant should coincide with the time constant, $\tau_c = \tau_{off}$, of the corresponding off-current. Even though the off-currents at pH values >7.5 are vanishingly small, the trend shown by the τ_{off} versus pH plot in Fig. 8 seems to support the above prediction. According to the expression of Eq. A4 for the off-current, the peak off-current should depend on b, but not on the resistance, R_p, of the SR membrane. In other words, the decrease in the pump stationary current b, up to its disappearance, with an increase in pH cannot be ascribed to the increase in R_p. It can be speculated that the countertransport of protons that occurs at physiological pH is fundamental for a correct turnover of Ca-ATPase, due to some molecular mechanism.

K^+ dependence of Ca^{2+} translocation

The presence of K^+ ion has been reported to affect the functioning of Ca-ATPase in different ways. Thus, it increases the rate of dephosphorylation of the P-E_2 form of Ca-ATPase (Shigekawa and Pearl, 1976; Chaloub and de Meis, 1980) and accelerates both the Ca^{2+} binding and dissociation in the absence of ATP (Moutin and Dupont, 1991; Orlowski and Champeil, 1991; Lee et al., 1995), suggesting that it increases the rate of the E_2–E_1 transition. Moreover, it has been proposed that Ca-ATPase catalyzes passive transport of K^+ when the protein is switched to its E_2 conformational state (Moutin and Dupont, 1991; de Jesus et al., 1995). Lee et al. (1995) interpreted the effect of K^+ on the binding of Ca^{2+} to Ca-ATPase by proposing the binding of K^+ to a ''gating'' site, in competition with Mg^{2+} and H^+, where it affects the affinity of the calcium pump for Ca^{2+}; they also postulated the binding of K^+ to the inner Ca^{2+} binding site, but not to the outer one. The fact that the charge after a 30 mM K^+ concentration jump in the absence of ATP is the same, both in the absence and in the presence of a saturating 100 μM free calcium concentration, strongly suggests that the K^+ binding site is distinct from the Ca^{2+} binding sites and that their occupancies do not interfere with each other. With respect to the charge after an ATP concentration jump in the presence of a saturating free calcium concentration and in the absence of K^+, the charge after a 30 mM K^+ concentration jump is ~40%, whereas that after the binding of the two Ca^{2+} ions in the absence of ATP is ~60% (see above). Since it is improbable that the K^+ ions may be translocated over a distance much greater than that of the Ca^{2+} ions in the membrane dielectric, it is reasonable to assume that K^+ binding to the cytoplasmic side of the pump involves more than one K^+ ion per pump. A number of binding sites for univalent ions on Ca-ATPase was indeed revealed by a study of Na^+ binding to SR using ^{23}Na NMR (Timonin et al., 1991).

In this connection, it is interesting to note from the inset of Fig. 9 that the presence of 30 mM K^+ decreases the peak current after Ca^{2+} translocation due to an ATP concentration jump by ~40%, whereas a further increase in the K^+ ion concentration may decrease it down to ~50%. Moreover, the concentration jump of both 100 μM ATP and 30 mM K^+ in Fig. 10 (*curve c*) clearly shows that the decrease in the charge to be ascribed to Ca^{2+} translocation with respect to the charge recorded in the absence of K^+ (compare *curves b* and *c*) is roughly equal to the charge initially involved in K^+ binding (compare *curves a* and *c*). This suggests that K^+ ions bind rapidly to specific binding sites other then the Ca^{2+} binding sites from the cytoplasmic side of the pump, when the latter is in the E_1 conformation, and are released rapidly to the same side during the E_1–E_2 conformational transition. This may explain the progressive decrease in the translocated charge after an ATP concentration jump with an increase in K^+ ion concentration, as shown in Fig. 9. Such an explanation is supported by the much higher affinity of K^+ for the cytoplasmic than for the lumenal side of Ca-ATPase (Lee et al., 1995). To confirm this point by our technique, a 30 mM K^+ concentration jump was carried out in a solution of 19 μM free calcium and 100 μM ATP, where the E_2 state of the pump prevails: no current transient was observed (data not shown).

The long tail exhibited by the current transients in Fig. 9 for K^+ concentrations ≥150 mM can be tentatively explained by an uncoupled downhill K^+ translocation due to a carrier-like pump operation, as proposed by Dupont and co-workers (Moutin and Dupont, 1991; de Jesus et al., 1995); in the presence of Ca^{2+}, this passive transport may only be observed at relatively high K^+ concentrations.

CONCLUSIONS

The current transients due to ATP, Ca^{2+}, and K^+ concentration jumps on SR vesicles adsorbed on a gold-supported mixed thiol/lipid bilayer allow a direct measurement of the charge translocated by Ca-ATPase under different activation conditions. Of the two relaxation times characterizing the descending branch of the on-current transients due to Ca^{2+} translocation induced by ATP concentration jumps, the shortest one, τ_1, is to be ascribed to an ATP binding step in

quasi-equilibrium followed by enzyme phosphorylation and a rate-determining release of bound Ca^{2+}. Conversely, the longest relaxation time, τ_2, responsible for a moderate current overshoot, is to be ascribed to a partial discharge of the capacitance of the SR membrane across its own resistance. The pH dependence of the charge due to Ca^{2+} translocation confirms unequivocally the countertransport of one H^+ per one Ca^{2+} at physiological pH; moreover, the progressive decrease of this countertransport in passing from pH 7 to pH 8 points to a cooperative binding of the two protons to the calcium pump. Upon comparing the charge involved in the binding of Ca^{2+} ions to the cytoplasmic side of the pump in the absence of ATP with that involved in Ca^{2+} translocation after an ATP concentration jump on the same SSM, it was possible to estimate the fractional distance of the Ca^{2+} binding sites from the cytoplasmic side at 0.32, in agreement with the highly resolved structures of Ca-ATPase (Toyoshima et al., 2000). The current transients after K^+ concentration jumps strongly suggest that, during an enzymatic cycle, K^+ ions bind to the cytoplasmic side of the calcium pump in the E_1 state and are released from the same side after the E_1–E_2 conformational transition.

APPENDIX

The analysis of the equivalent circuit of Fig. 13 yields the two differential equations:

$$I = -I_p G(t,T) - C_p\frac{dv_p}{dt} - \frac{v_p}{R_p} \quad \text{(a)};$$
$$I = -\frac{v_m}{R_m} - C_m\frac{dv_m}{dt} \quad \text{(b)}. \tag{A1}$$

Here, I is the current, taken as positive when it flows from the solution toward the electrode along the external circuit. I_p is the pump current, v_p and v_m are the potential differences between A and B and between B and C, T is the activation period, and $G(t,T)$ is a gate function. The differential equation for v_m, as obtained by eliminating I between the above two equations, substituting I_p from Eq. 4, and setting $v_p = E - v_m$, is solved by the use of the Laplace transforms. The resulting expression of v_m is then substituted into Eq. A1b yielding:

$$I(t) = -\frac{E}{R_m+R_p} - \frac{C_m}{C_m+C_p}\left[\sum_i a_i\frac{\tau_c(\tau_m-\tau_i)}{\tau_m(\tau_c-\tau_i)}e^{-t/\tau_i} + \left(b - \sum_i a_i\frac{\tau_i}{\tau_c-\tau_i}\right)\frac{\tau_m-\tau_c}{\tau_m}e^{-t/\tau_c} + b\frac{\tau_c}{\tau_m}\right] \quad \text{for} \quad t<T \tag{A2}$$

$$I(t) = -\frac{E}{R_m+R_p} + \frac{C_m}{C_m+C_p}\frac{\tau_m-\tau_c}{\tau_m} \times \left[\sum_i a_i\frac{\tau_i}{\tau_c-\tau_i}\left(e^{-\frac{t}{\tau_c}} - e^{-\frac{T}{\tau_i}-\frac{(t-T)}{\tau_c}}\right) + b\left(e^{-\frac{(t-T)}{\tau_c}} - e^{-\frac{t}{\tau_c}}\right)\right] \quad \text{for} \quad t>T \tag{A3}$$

$$\text{with}: \quad \tau_m = R_mC_m; \quad \tau_c = (C_p+C_m)\frac{R_mR_p}{R_m+R_p}.$$

These equations are obtained by noting that $v_m(t=0) = R_mE/(R_m+R_p)$. The term $-E/(R_m+R_p)$ is the constant current that flows along the external current both in the absence and in the presence of activation of the pump: for sufficiently high R_m values it becomes vanishingly small, causing the current to become independent of the applied potential. The experimental stationary current due to the pump stationary current b is equal to $-C_m(\tau_c/\tau_m)b/(C_m+C_p)$, and becomes vanishingly small for $\tau_m \gg \tau_c$. Under usual experimental conditions, $\tau_m \gg \tau_c$ and the activation period T is much greater than both τ_c and τ_i. Consequently, all exponential functions with exponent $-t/\tau_c$ and $-T/\tau_i$ in Eq. A3 are negligibly small and this equation assumes the simplified form

$$I(t) = \frac{C_m}{C_m+C_p}b\,e^{-\frac{t-T}{\tau_c}} \quad \text{for} \quad t>T. \tag{A4}$$

The time dependence of the concentration c of the activating substance that comes in contact with the SSM is approximately expressed by the equation (Pintschovius and Fendler, 1999)

$$c(t) = c_0[t/(t+\tau_{app})], \tag{A5}$$

where c_0 is the concentration of the activating substance in the container connected to the cuvette of the SSM via the solenoid valve, and τ_{app} is an empirical parameter. To verify the effect of the resulting noninstantaneous concentration jump on the current transient, let us consider the simple irreversible process consisting in the binding of a ligand L to a pump P:

$$L + P \xrightarrow{k} LP \quad \text{with}: [P] + [LP] = [P_t], \tag{A6}$$

where $[P_t]$ is the total concentration of the pump. The current transient is proportional to

$$\frac{dx}{dt} = kc_0\frac{t}{t+\tau_{app}}(1-x) \quad with: x \equiv \frac{[LP]}{[P_t]}. \tag{A7}$$

Numerical solution of this differential equation with the fourth order Runge-Kutta method for $\tau_{app} = 90$ ms yields dx/dt versus t curves with the typical shape of the current transients in Figs. 1, 7, and 9. To extract a quantity proportional to the rate constant kc_0 from these calculated curves, two alternative procedures can be followed: i), measuring the peak current, I_{peak}, and ii), fitting the decaying branch of the current transient with a monoexponential function, starting from the time, t_{peak}, of the current peak taken as the origin, and determining the reciprocal of the resulting relaxation time constant, τ. Fig. 14 shows plots of I_{peak} and τ^{-1} versus kc_0. The I_{peak} versus kc_0 plot shows a curvature for $kc_0 < 7$ 5 s^{-1}, whereas it is practically linear from 75 to over 350 s^{-1} (not shown in the figure). On the

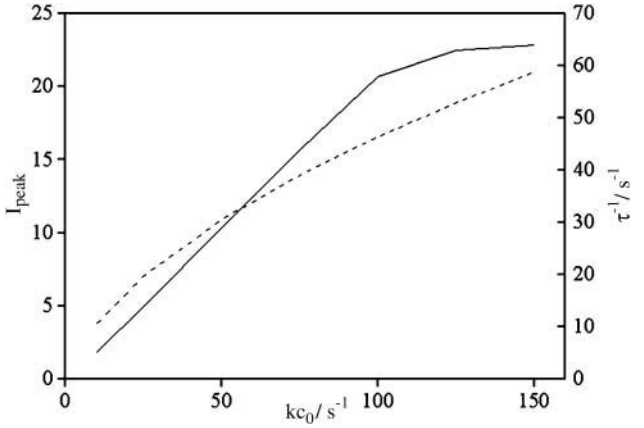

FIGURE 14 Plots of I_{peak} (*dotted line*) and τ^{-1} (*solid line*) versus kc_0. For the meaning of the parameters, see the Appendix.

other hand, the τ^{-1} versus kc_0 plot is perfectly linear and passes through the origin, but tends to a saturation value when kc_0 approaches t_{peak}^{-1}. This is clearly to be expected, because under these conditions the relaxation time of the process becomes masked by the noninstantaneous increase in the concentration, $c(t)$, of the activating substance in contact with the SSM.

The authors thank Dr. Giovanni Aloisi for the preparation of the gold thin films.

Thanks are due to the Ente Cassa di Risparmio di Firenze, to the Ministero dell'Istruzione, dell'Università e della Ricerca and to the CNR (National Council for Scientific Research)-Agenzia 2000 for financial support.

REFERENCES

Bamberg, E., H. J. Apell, N. A. Dencher, W. Sperling, H. Stieve, and P. Läuger. 1979. Photocurrents generated by bacteriorhodopsin on planar bilayer membranes. *Biophys. Struct. Mech.* 5:277–292.

Bers, D. M., C. W. Patton, and R. Nuccitelli. 1994. A practical guide to the preparation of Ca^{2+} buffers. *In* Methods in Cell Biology, Vol. 40: A Practical Guide to the Study of Calcium in Living Cells. R. Nuccitelli, editor. Academic Press, San Diego, CA. Ch. 1.

Borlinghaus, R., H.-J. Apell, and P. Läuger. 1987. Fast charge translocations associated with partial reactions of the Na,K pump. I. Current and voltage transients after photochemical release of ATP. *J. Membr. Biol.* 97:161–178.

Butscher, C., M. Roudna, and H. J. Apell. 1999. Electrogenic partial reactions of the SR-Ca-ATPase investigated by a fluorescence method. *J. Membr. Biol.* 168:169–181.

Carafoli, E., and M. Brini. 2000. Calcium pumps: structural basis for and mechanism of calcium transmembrane transport. *Curr. Opin. Chem. Biol.* 4:152–161.

Chaloub, R. M., and L. de Meis. 1980. Effect of K^+ on phosphorylation of the sarcoplasmic reticulum ATPase by either P_i or ATP. *J. Biol. Chem.* 255:6168–6172.

de Jesus, F., M. Cuillel, and Y. Dupont. 1995. Evidence for direct involvement of the sarcoplasmic reticulum Ca-ATPase in a passive monovalent cation (K^+/Na^+) exchange. *FEBS Lett.* 376:167–171.

Deranleau, D. A. 1969. Theory of the measurement of weak molecular complexes. II. Consequences of multiple equilibria. *J. Am. Chem. Soc.* 91:4050–4054.

Dolfi, A., F. Tadini Buoninsegni, M. R. Moncelli, and R. Guidelli. 2002. Photocurrents generated by bacteriorhodopsin adsorbed on thiol/lipid bilayers supported by mercury. *Langmuir.* 18:6345–6355.

Dupont, Y., and J. B. Leigh. 1978. Transient kinetics of sarcoplasmic reticulum Ca^{2+},Mg^{2+}-ATPase studied by fluorescence. *Nature.* 273: 396–398.

Eletr, S., and G. Inesi. 1972. Phospholipid orientation in sarcoplasmic membranes: spin-label ESR and proton MNR studies. *Biochim. Biophys. Acta.* 282:174–179.

Fendler, K., S. Jaruschewski, A. Hobbs, W. Albers, and J. P. Froehlich. 1993. Pre-steady-state charge translocation in NaK-ATPase from eel electric organ. *J. Gen. Physiol.* 102:631–666.

Florin, E. L., and H. E. Gaub. 1993. Painted supported lipid membranes. *Biophys. J.* 64:375–383.

Ganea, C., T. Pourcher, G. Leblanc, and K. Fendler. 2001. Evidence for intraprotein charge transfer during the transport activity of the melibiose permease from *Escherichia coli*. *Biochemistry.* 40:13744–13752.

Gommans, I. M. P., M. H. M. Vlak, A. de Haan, and B. G. M. van Engelen. 2002. Calcium regulation and muscle disease. *J. Muscle Res. Cell Motil.* 23:59–63.

Hartung, K., J. P. Froehlich, and K. Fendler. 1997. Time-resolved charge translocation by the Ca-ATPase from sarcoplasmic reticulum after an ATP concentration jump. *Biophys. J.* 72:2503–2514.

Hartung, K., E. Grell, W. Hasselbach, and E. Bamberg. 1987. Electrical pump currents generated by the Ca-ATPase of sarcoplasmic reticulum vesicles adsorbed on black lipid membranes. *Biochim. Biophys. Acta.* 900:209–220.

Henderson, I. M. J., Y. M. Khan, J. M. East, and A. G. Lee. 1994. Binding of Ca^{2+} to the (Ca^{2+}-Mg^{2+})-ATPase of sarcoplasmic reticulum: equilibrium studies. *Biochem. J.* 297:615–624.

Hua, S., H. Ma, D. Lewis, and G. Inesi. 2002. Functional role of ''N'' (nucleotide) and ''P'' (phosphorylation) domain interactions in the sarcoplasmic reticulum (SERCA) ATPase. *Biochemistry.* 41:2264–2272.

Inesi, G. 1987. Sequential mechanism of calcium binding and translocation in sarcoplasmic reticulum adenosine triphosphatase. *J. Biol. Chem.* 262:16338–16342.

Inesi, G., M. Kurzmack, C. Coan, and D. E. Lewis. 1980. Cooperative calcium binding and ATPase activation in sarcoplasmic reticulum vesicles. *J. Biol. Chem.* 255:3025–3031.

Inesi, G., M. Kurzmack, and D. Lewis. 1988. Kinetic and equilibrium characterization of an energy-transducing enzyme and its partial reactions. *Methods Enzymol.* 157:154–190.

Inesi, G., C. Sumbilla, and M. E. Kirtley. 1990. Relationships of molecular structure and function in Ca^{2+}-transport ATPase. *Physiol. Rev.* 70:749–760.

Ishii, T., F. Hata, M. V. Lemas, D. M. Fambrough, and K. Takeyasu. 1997. Carboxy-terminal regions of the sarcoplasmic/endoplasmic reticulum Ca^{2+}- and the Na^+/K^+-ATPases control their K^+ sensitivity. *Biochemistry.* 36:442–451.

Läuger, P. 1991. Electrogenic Ion Pumps. Sinauer Associates, Sunderland, MA.

Lee, A. G., K. Baker, Y. M. Khan, and J. M. East. 1995. Effects of K^+ on the binding of Ca^{2+} to the Ca-ATPase of sarcoplasmic reticulum. *Biochem. J.* 305:225–231.

Lee, A. G., and J. M. East. 2001. What the structure of a calcium pump tells us about its mechanism. *Biochem. J.* 356:665–683.

MacLennan, D. H. 2000. Ca^{2+} signaling and muscle disease. *Eur. J. Biochem.* 267:5291–5297.

Møller, J. D., B. Juul, and M. le Maire. 1996. Structural organization, ion transport, and energy transduction of P-type ATPases. *Biochim. Biophys. Acta.* 1286:1–51.

Moutin, M.-J., and Y. Dupont. 1991. Interaction of potassium and magnesium with the high affinity calcium-binding sites of the sarcoplasmic reticulum calcium-ATPase. *J. Biol. Chem.* 266:5580–5586.

Orlowski, S., and P. Champeil. 1991. Kinetics of calcium dissociation from its high-affinity transport sites on sarcoplasmic reticulum ATPase. *Biochemistry.* 30:352–361.

Peinelt, C., and H.-J. Apell. 2002. Kinetics of the Ca^{2+}, H^+, and Mg^{2+} interaction with the ion-binding sites of the SR Ca-ATPase. *Biophys. J.* 82:170–181.

Peinelt, C., and H.-J. Apell. 2004. Time-resolved charge movements in the sarcoplasmatic reticulum Ca-ATPase. *Biophys. J.* 86:815–824.

Pintschovius, J., E. Bamberg, and K. Fendler. 1999. Charge translocation by the Na^+/K^+-ATPase investigated on solid supported membranes: cytoplasmic cation binding and release. *Biophys. J.* 76:827–836.

Pintschovius, J., and K. Fendler. 1999. Charge translocation by the Na^+/K^+-ATPase investigated on solid supported membranes: rapid solution exchange with a new technique. *Biophys. J.* 76:814–826.

Seifert, K., K. Fendler, and E. Bamberg. 1993. Charge transport by ion translocating membrane proteins on solid supported membranes. *Biophys. J.* 64:384–391.

Shigekawa, M., and L. J. Pearl. 1976. Activation of calcium transport in skeletal muscle sarcoplasmic reticulum by monovalent cations. *J. Biol. Chem.* 251:6947–6952.

Sreter, F. A. 1963. Cell water, sodium, and potassium in stimulated red and white mammalian muscles. *Am. J. Physiol.* 205:1295–1298.

Tadini Buoninsegni, F., P. Nassi, C. Nediani, A. Dolfi, and R. Guidelli. 2003. Investigation of Na^+,K^+-ATPase on a solid supported membrane:

the role of acylphosphatase on the ion transport mechanism. *Biochim. Biophys. Acta*. 1611:70–80.

Tadini Buoninsegni, F., J. Pintschovius, F. Cornelius, E. Bamberg, and K. Fendler. 2000. K^+ induced charge translocation in the phosphoenzyme formed from inorganic phosphate. *In* Na^+,K^+-ATPase and Related ATPases. K. Taniguchi and S. Kaya, editors. Elsevier, Amsterdam. 341–348.

Timonin, I. M., S. N. Dvoryantsev, V. V. Petrov, E. K. Ruuge, and D. D. Levitsky. 1991. Interaction of alkaline metal ions with Ca^{2+}-binding sites of Ca-ATPase of sarcoplasmic reticulum: ^{23}Na-NMR studies. *Biochim. Biophys. Acta*. 1066:43–53.

Toyoshima, C., M. Nakasako, H. Nomura, and H. Ogawa. 2000. Crystal structure of the calcium pump of sarcoplasmic reticulum at 2.6 Å resolution. *Nature*. 405:647–655.

Toyoshima, C., and H. Nomura. 2002. Structural changes in the calcium pump accompanying the dissociation of calcium. *Nature*. 418:605–611.

Yamada, S., and N. Ikemoto. 1980. Reaction mechanism of calcium-ATPase of sarcoplasmic reticulum. *J. Biol. Chem*. 255:3108–3119.

Yoshimura, S. H., T. Ishii, J. C. Yasuhara, M. H. Sato, and K. Takeyasu. 1997. Ion-sensitive domains of the SERCA- and the Na^+/K^+-ATPases identified by chimeric recombination. *Ann. N. Y. Acad. Sci*. 834:588–591.

Yu, X., S. Carroll, J. L. Rigaud, and G. Inesi. 1993. H^+ countertransport and electrogenicity of the sarcoplasmic reticulum Ca^{2+} pump in reconstituted proteoliposomes. *Biophys. J*. 64:1232–1242.

Yu, X., L. Hao, and G. Inesi. 1994. A pK change of acidic residues contributes to cation countertransport in the Ca-ATPase of sarcoplasmic reticulum. *J. Biol. Chem*. 269:16656–16661.